Desalination and Water Treatment
www.deswater.com

doi: 10.5004/dwt.2022.28591

265 (2022) 18–26
July

A sustainable approach to repurpose discarded air filter for extended use in oil/water separation

Jian-Hua Wei[a], Xiangchen Li[a], Wei-Guo Yan[a,b,c,*], Congcong Shen[c], Zhifeng Liu[a,b,*]

[a]*School of Materials Science and Engineering, Tianjin Chengjian University, Tianjin 300384, China, emails: yan_weiguo@163.com (W.-G. Yan), tjulzf@163.com (Z. Liu), wei_jianhua132@163.com (J.-H. Wei), 1271522205@qq.com (X. Li)*
[b]*Tianjin Key Laboratory of Building Green Functional Materials, Tianjin Chengjian University, Tianjin 300384, China*
[c]*School of Science, Tianjin Chengjian University, Tianjin 300384, China, email: ccshen2021@126.com (C. Shen)*

Received 29 September 2021; Accepted 19 May 2022

ABSTRACT

With increasing automobiles in the past decade, more and more discarded air filters (DAFs) have caused severe environmental pollution due to automobile maintenance. We proposed an efficient and simple method for preparing superhydrophobic/superoleophilicity air filter for oil/water separation to solve this problem. The DAFs were functionalized by polydimethylsiloxane (PDMS) and titanium dioxide nanoparticles to enhance its hydrophobicity and oleophilicity. The morphological study showed that the use of PDMS as a binder changed the surface structure of the coatings significantly. Oil/water separation experiments revealed that DAFs could separate various oils with separation efficiencies exceeding 99%. Importantly, Experiments have shown that the superhydrophobic/oleophilic air filter cartridge maintains a high separation efficiency (>96%) after at least ten filter cycles under oil-water mixtures with alkaline, acidic, and saline solutions. The superoleophobicity of DAFs was maintained in solutions of alkaline, acidic, and saline solutions for at least 72 h, indicating good durability and stability. More importantly, the DAFs not only removes oil from oily wastewater (such as in tanker leaks) but also realizes secondary use.

Keywords: Superhydrophobic; Superoleophilicity; Discard air filters; Ecologically beneficial; TiO_2 nanoparticles

1. Introduction

Due to the increasing quantity of oily industrial wastewater and the increasing frequency of oil spill incidents, oil/water separation has received a great deal of attention in recent years [1–6]. For this reason, environmental concerns, stringent environmental laws, and the need for clean technology have improved the separation standard of oil/water mixtures. In the past, oil/water separation technology has solved many waste disposal problems and boosted the purification of water, soil, and atmosphere. Due to the rapid growth of cars, there are a large number of discarded air filters (DAFs), which resulted in environmental damage. The traditional treatment methods of DAFs include landfilling and incineration [7–9]. However, the methods still existed second pollution.

The reutilization of DAFs has become a very important issue. Due to their good porosity and mechanical and chemical stability, the DAFs can not only filter small particles in the air, but also adsorb pollutants in water, or oil/water mixture. For example, some porous structures including waste nanofibers [10–12], waste paper [13–17], fabric [18–20], waste wood [21–24], waste cigarette filter [25–28], etc., have used for oil/water separation. Although some researches have been carried out on the superhydrophobicity of fabric and waste fibers, there are not still reported the studies on DAFs for oil/water separation. However, DAFs achieved high efficient oil-water separation due to

* Corresponding authors.

their surface hydrophilicity. Consequently, designing functionalized DAFs with superhydrophobic and lipophilic properties is a key factor.

Over the last 10 y, titanium dioxide (TiO_2) nanoparticles have become a research hotspot for constructing rough surfaces due to the stable physicochemical properties, excellent optical properties, and photochemical activity [29–32]. According to the special wettability theories [33,34], nano-roughness structure and low surface free energy materials have been mainly used to fabricate superhydrophobic coatings on different substrates. Considering the environmental friendliness and chemical stability, TiO_2 nanoparticles were coated on the surface through immersion treatment and heat curing, which exhibited superhydrophobicity [35]. For instance, Khanjani et al. [36] produced superhydrophobic paper by spin-coating a dispersion of nanostructured fluorinated cellulose esters. Qiu et al. [37] developed excellent superwetting stainless steel meshes by spraying silicon dioxide nanoparticles modified by hexadecyltrimethoxysilane onto the stainless steel meshes. However, due to its potential hazards to flora and fauna, and the environment, fluorides have been prohibited for use by most of the world [38]. Therefore, using TiO_2 nanoparticles with rough surface and Polydimethylsiloxane (PDMS) with low surface energy to modify DAFs, this is an economical and environmental method to achieve oil-water separation.

The main objective of this research is to investigate TiO_2 nanoparticles and PDMS modified DAFs for oil-water separation. PDMS, as a good abrasion resistance material, can bond tightly to the surface of various DAFs without adding any fluorides additives [40]. Modified DAFs showed durable superhydrophobic in different environment and the water contact angle (WCA) reached 150°. In addition, Modified DAFs achieved high efficient oil-water separation in oil spill clean-up. This method will provide an effective and low-cost strategy for practical applications in oil-water separation.

2. Experimental section

2.1. Materials

TiO_2 (average particle size of 2 to 10 nm) and the ethyl acetate are purchased from Tianjin Kermel Chemical Reagent Co., Ltd. (China). PDMS and ethyl acetate were purchased from Dow Corning Co., USA. Different types of DAFs were purchased from a local market. China National Petroleum Corporation provided diesel oil (CNPC) and motor oil. Soybean oil is purchased from local supermarkets. Kaitong Chemical Reagent Co. (China) supplied the Sudan Red III and Indigo.

2.2. Preparation of DAFs coated membranes

Firstly, the collected DAFs (Fig. 4a) were washed with hot water several times. Before the coating process, the as-received DAFs were first to cut into 30 mm^2 × 50 mm^2, then cleaned ultrasonically in ethanol for 20 min to remove any surface impurities, and then washed with distilled water. 0.1 g TiO_2 nanoparticles were scattered in 30 mL ethyl acetate, and 0.5 g PDMS was dissolved in the above solution. Afterward, the 0.05 g curing agent was added to the suspension and stirred for 10 min. The addition of PDMS can enhance the binding force between the TiO_2 nanoparticles and the DAFs skeleton. Four clean DAFs were immersed in the above solution for an optimal time of 30 min. Then, the obtained coatings were dried entirely at room temperature to remove residual ethyl acetate. Contents of TiO_2 nanoparticles and PDMS were determined as given in Table 1. Finally, the procedures above were applied to four different DAFs.

2.3. Immiscible oil/water mixtures separation

The DAFs are held in place by two 2.5-cm-diameter glass tubes. In this test, two types of soybean oil and motor oil were used. Indigo and oil red were used to color the water and oil, respectively. The density used oils are listed in Table 2. A water/oil mixture (50% v/v) was poured onto a wetted sample surface. When light oil and water were separated, the modified DAFs were prewetted with water before separation; similarly, the modified DAFs were prewetted with oil before heavy oil and water (water-oil) separation. Eq. (1) was used to calculate separation efficiency.

$$\left(\partial\right) = \left(1 - \frac{c_e}{c_f}\right) \times 100 \tag{1}$$

where c_f denotes the oil content before separation and c_e denotes the concentration of recovered oil after separation.

2.4. Preparation and separation of oil-in-water emulsions

Emulsion separation experiments were carried out under vacuum filtration using SCJ-10 vacuum pump (SUPO Co., China). Four types of DAFs were measured in order to find out which had the best separation effect. The separation experiments were carried out at room temperature and pressure of 15 mm Hg. Finally, the oil droplet size were measured filtration using the total organic analyzer (XU65-TOC-2000).

Table 1
PDMS and TiO_2 dosage for four samples

Samples	TiO_2 (wt.%)	SiO_2 (wt.%)
Toyota Prado	0.1	0.5
Corolla	0.1	0.5
Santana	0.5	0.5
Volkswagen	0.3	0.5

Table 2
Physical properties of test oils and solvents

Miscellaneous oil	Density (g/cm^3)
Diesel	0.820–0.845
Soybean oil	0.915–0.938
Motor oil	0.910
Chloroform	1.47

2.5. Characterization

Scanning electron microscopy (SEM) images and energy-dispersive X-ray spectroscopy (EDX) maps were taken using Zeiss Merlin Compact to optimize the experimental conditions. The elemental and chemical composition of the DAFs are characterized by an ESCALAB 250Xi X-ray Photoelectron Spectrometer (XPS, Thermo Scientific, USA) and Fourier-transform infrared spectroscopy (FTIR, Bruker VERTEX 33, Germany). A contact angle meter (DropMeter™ Element A-60) was used to evaluate the wettability, and each data point was produced by taking the average of five repeated measurements. The optical microscope was used to collect and examine the scattered droplets in the emulsions (Leica DVM6s). The oil content was measured by the total organic analyzer (XU65-TOC-2000).

3. Results and discussion

3.1. Composition analysis and morphologies of samples

A superhydrophobic DAFs have been successfully prepared by integrating TiO_2 nanoparticles with PDMS adhesive. The detailed preparation methods are illustrated schematically in Fig. 1. Initially, the PDMS was dispersed in ethyl acetate solvent to obtain the mixture solutions. After that, DAFs were dipped in ethyl acetate and PDMS mixture. After evaporation of ethyl acetate, DAFs with superhydrophobic coating were prepared.

SEM was used to study the surface morphology of the different DAFs. Fig. 2a shows that four different DAFs exhibited porous and interconnected three-dimensional (3D) network with tightly cross-linked fibers with an average pore size of around 35 μm. From magnified SEM in Fig. 2b, it is not difficult to see that there are the PDMS and TiO_2 on DAFs surface, which is crucial for forming stable superhydrophobic and oleophilic. In addition, the holes of fibrous structures have been almost covered by PDMS and TiO_2 after dipping. Fig. 2c is EDX mapping of the DAFs surface coated with PDMS/TiO_2, which confirmed the presence of C, Si, O, Ti elements.

To further verify DAFs modified with PDMS and PDMS/TiO_2 respectively, the FTIR spectra were investigated in Fig. 3a. The –OH stretching vibration is responsible for developing the peak between 3,300 and 3,700 cm^{-1}. Asymmetric $–CH_3$ stretching, symmetric $–CH_3$ deformation, and $–CH_3$ rocking in $Si–CH_3$ of PDMS have peaks at

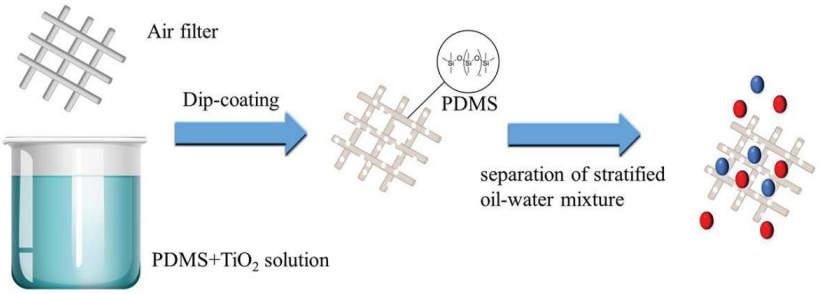

Fig. 1. Schematic description of the preparation of DAFs coated with PDMS/TiO_2 nanocomposites and the oil/water separation process.

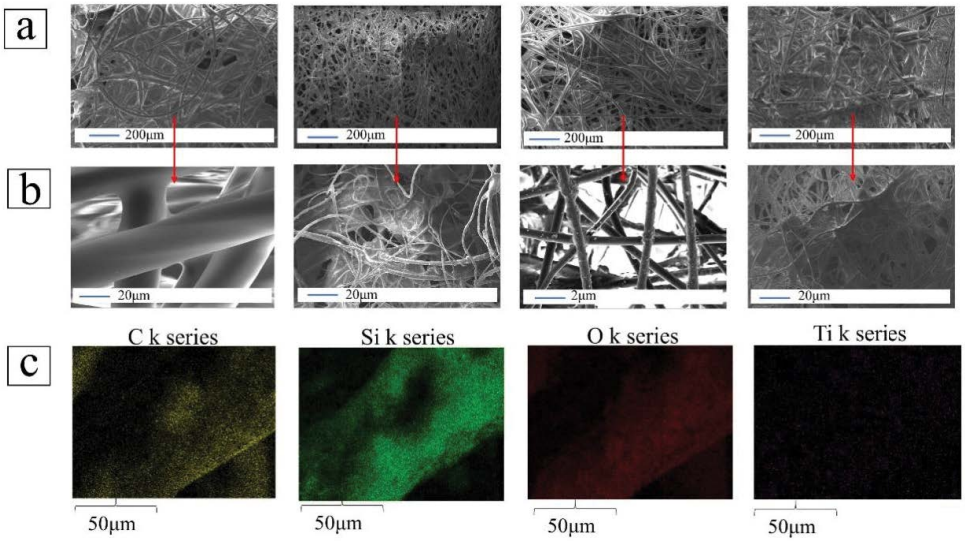

Fig. 2. Surface morphology of (a) coated four types of air filter elements (b), the PDMS/TiO_2 air filters of different magnification, and (c) energy-dispersive X-ray spectroscopy results of the PDMS/TiO_2 air filters.

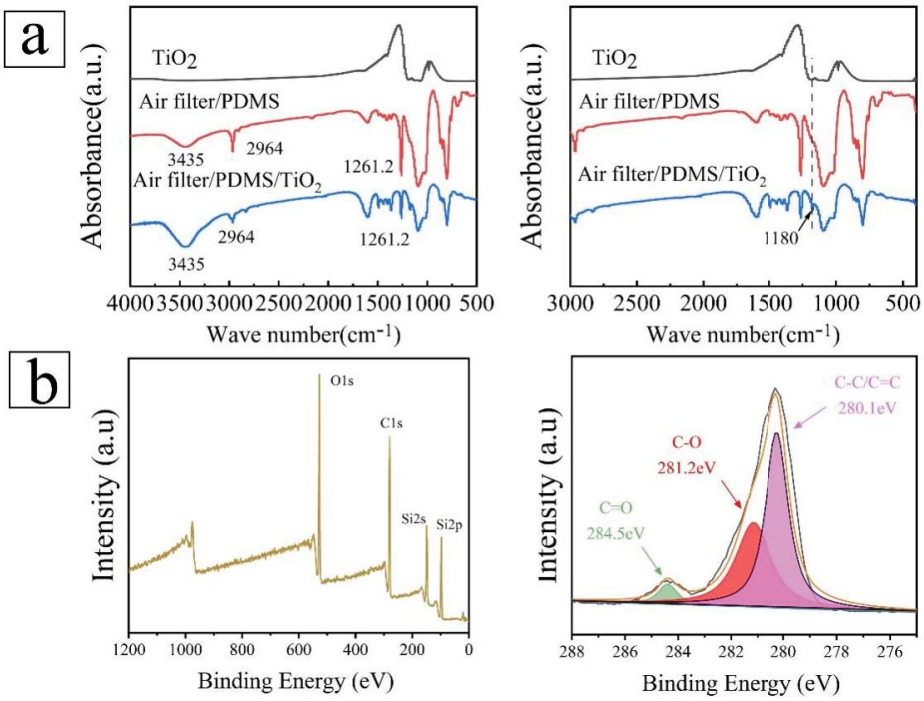

Fig. 3. (a) FTIR spectra of TiO_2 powder, DAF/PDMS, and DAF/PDMS/TiO_2 samples and (b) XPS analysis of DAF coated with PDMS/TiO_2 formulation.

roughly 2,964; 1,261.2, and 802.2 cm^{-1}. The asymmetric Si–O–Si stretching vibration absorption has a broad, multicomponent peak extending from 930 to 1,200 cm^{-1}. Compared to the PDMS modified DAFs, the spectra of PDMS and TiO_2 modified DAFs showed that absorption bands was at about 1,180 cm^{-1}, which is attributed to TiO_2 crystal vibration absorption peaks.

The surface chemistries of DAFs coated with PDMS/TiO_2 were analyzed using XPS in Fig. 3b. Two peaks appeared at 98 and 149 eV, which were related to Si_{2p} and Si_{2s}, respectively. However, the peaks related to the TiO_2 were not detected, which is not unexpected due to the lack of surface penetration of XPS measurements.

3.2. Surface wettability of PDMS and TiO_2 coated DAFs

The four types of DAFs and corresponding sample sizes are shown in Fig. 4a. To test the hydrophobicity of the modified DAFs, the contact angle were carried out. Water droplets can be repelled from the coating surface by the Cassie–Baxter state owing to the micro-nano structure formed by TiO_2 nanoparticles combined with the low surface energy of the PDMS covering, and all testing water droplets on the modified DAFs are superhydrophobic with WCAs over 150°, as shown in Fig. 4b. Considering the stability of superhydrophobic coatings in various harsh environments, the modified DAFs were tested at different pH (from pH = 0 to pH = 14). Fig. 4c and d show the change of contact angle. The results showed that the superhydrophobic function of the modified DAFs did not decline significantly after dripping for 5 h.

As shown in Fig. 5b and d, the original and modified DAFs were immersed in water and gently pressed. The original air filter sample quickly sank to the bottom of the beaker. The modified DAFs still floats on the water surface after adding the weight of a key in Fig. 5e. Fig. 5f shows the WCA of the modified DAFs with a contact angle greater than 130°. It is also worth noting that proper micro-nanoscale porosity and coating thickness can keep low-surface tension liquid droplets on the surface.

3.3. Motor oil absorption test

Fig. 6a shows the oil absorption test of DAFs with a mixture of motor oil and water. Motor oil (oil red-stained) forms a red layer on the water's surface. It can be noticed that the superhydrophobic DAFs floats on top of the mixture and quickly collects the motor oil. After about 2 min, the superhydrophobic DAFs absorbed most of the oil. As shown in Fig. 6b, the modified DAFs still retained the superhydrophobicity after ten cycles, which indicated the effective recyclability of the PDMS-TiO_2 DAFs. As a result, the oil/water mixture can only be separated on-demand by the as-prepared PDMS-TiO_2 DAFs with excellent efficiency through a simple and low-cost fabrication method. In addition, taking a motor oil-water mixture as an example, the connection between oil-water separation efficiency and cycle count was investigated. The separation efficiency of modified DAFs was determined to be greater than 96% after 10 cycles. Fig. 6c shows that the modified air filter element has excellent reusability. As demonstrated in Fig. 2, the PDMS coating acts as a binder at the nanoparticle-substrate interface, firmly cementing

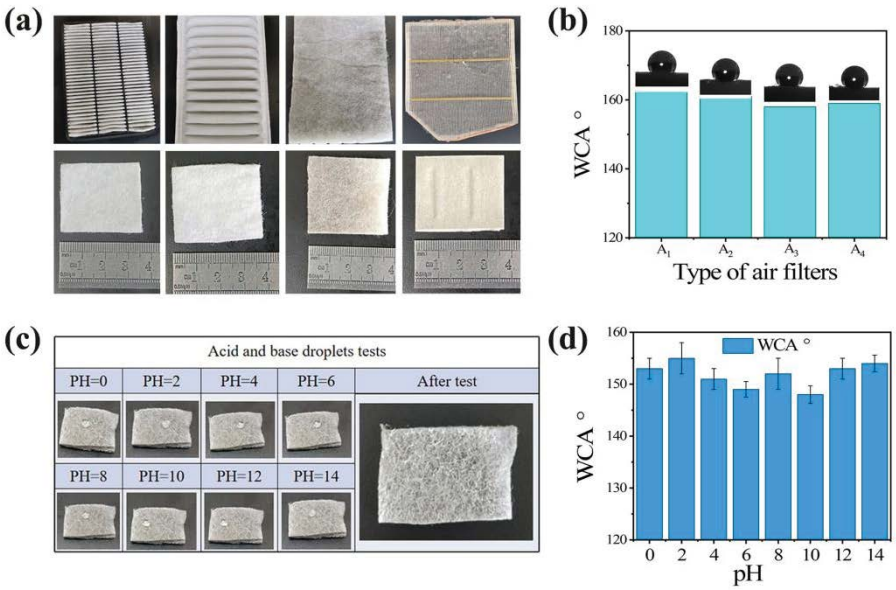

Fig. 4. Digital photograph of four common air filter elements from a car filter: (a,b) shows four types of modified air filter elements, respectively. The WCAs were more extensive than 154°, indicating that the modified DAFs were superhydrophobic below oil-water systems. Effects of (c) testing pH on WCAs of the surface of the class of DAFs with the most considerable porosity. (d) Shows the variation of the air filter with different pH in WCAs.

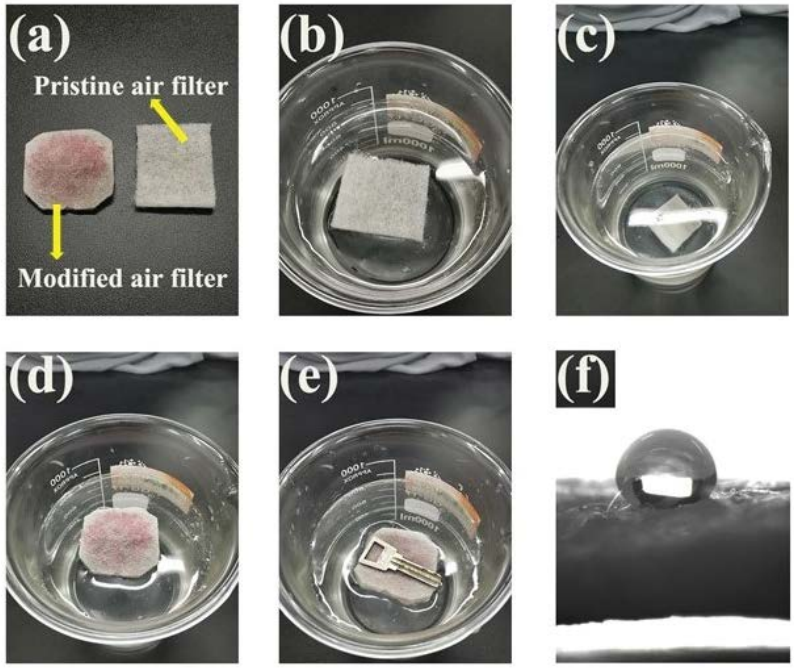

Fig. 5. (a) The pristine air filter sample and superhydrophobic modified air filter sample. (b) The pristine air filter sample and (c) superhydrophobic air filter sample float freely on the water. (d) The pristine air filter sample without loading. (e) The superhydrophobic air filter sample with loading of 0.645 g. (f) The WCA of modified air filter sample.

the nanoparticles and preventing them from slipping off the surface even after repeated compression. As illustrated in Fig. 6c, the aforesaid result illustrated the effective recyclability of DAFs. More importantly, the material appeared robust mechanical durability due to the strong bonding force between the filter skeletons and the PDMS. The modified DAFs could successfully separate immiscible oil/water solutions (heavy oil/water and light oil/water mixes).

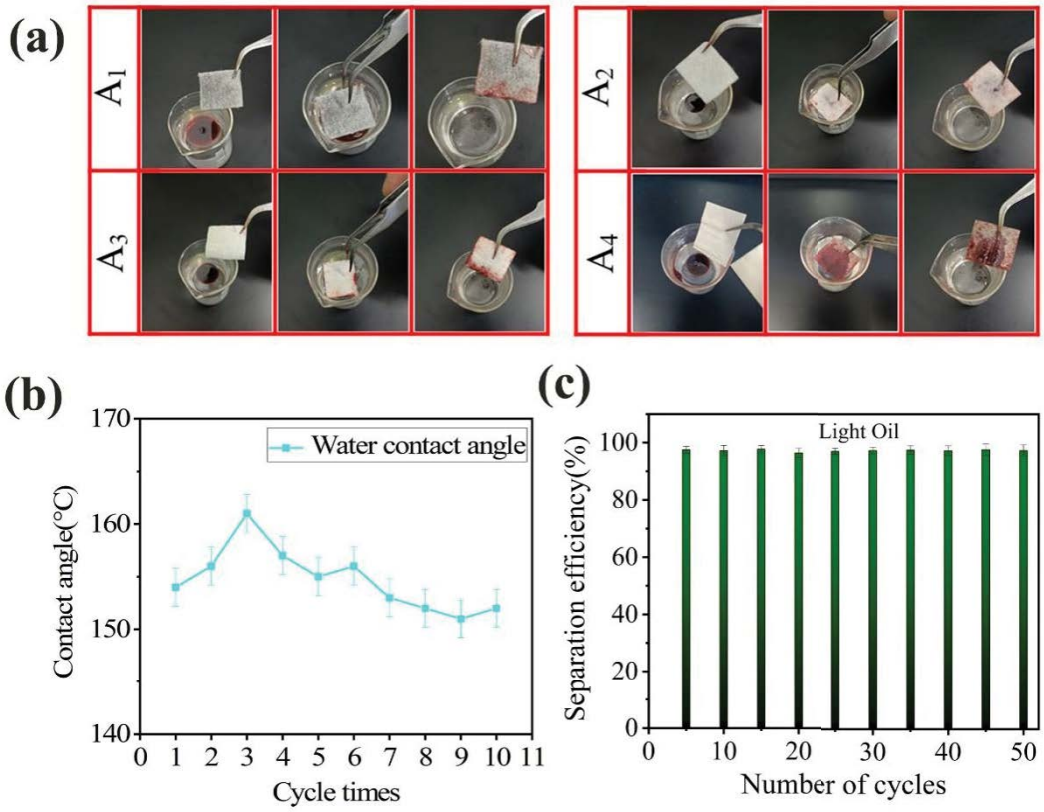

Fig. 6. (a) Digital photographs of oil-water separation using modified DAFs. (b) The average WCA of modified air filter in each cycle of oil-water separation. (c) The cycling stability of the DAF for oil/water separation.

The emulsion separation performance of the air filter was a critical aspect in the treatment of oily water. To evaluate the emulsion separation performance of the modified DAFs, the separation tests of two emulsions (including soybean oil and motor oil emulsions) were carried out. The motor oil/water emulsion was yellow, as shown in Fig. 7a, and the oil droplets could be readily detected using an optical microscope. It was discovered that the average size of oil droplets distributed emulsion feeds was less than 10 μm. At the same time, the filtrate was fully transparent and had no noticeable oil droplets, which indicated that the modified DAFs were capable of separating the emulsions effectively. Meanwhile, the soybean oil/water emulsion color was non-transparent, as illustrated in Fig. 7b, and the milky white phenomena were observed. According to the optical microscope snapshot, all water droplets are in the 10-micron size range. The filtrate obtained after separation by the modified DAFs was colorless and transparent, with no oil droplets visible in the optical microscope image of the filtrate (Fig. 7b).

The separation processes of the oil-water mixture, driven by gravity, are depicted in Fig. 8a–d. Various air filter (Toyota Prado, Corolla, Santana, and Volkswagen) sample was fixed between the filter cup and the conical flask to separate oil-water mixture. Because the captured oil prevented water from passing through the modified DAFs pouring, the water remained above the air filter, resulting in the complete separation of the oil and water mixtures. The separation capabilities of the TiO_2/PDMS modified DAFs for both mixtures were assessed by the filtrate flux and associated separation efficiencies to define the separation capabilities. The oil flux influences oil/water mixture separation speed and efficiency. $F = V/S$, where V represents the volume of oil flowing through the air filter, S represents the liquid's contact area with the air filter. As demonstrated in Fig. 8e, the average oil flux of the four DAFs was measured at the standard vertebral atmospheric pressure. Santana-type air filter showed the highest oil flux of 2,3081 L/m^2 h, while the other air filter (Volkswagen) was much lower (18,579 L/m^2 h). The permeating flux of the Remaining air filter was calculated as 19,562 and 21,067 L/m^2 h. This implies that the various air filter types significantly influence the penetration. Oil-water mixtures were studied using soybean oil and motor oil as the oil phase to measure air filter effectiveness for separating two oil-water combinations further. The separation efficiency (β) was assessed according to Eq. (2).

$$\beta = \left(\frac{m_2}{m_1}\right) \times 100\% \tag{2}$$

where m_2 is the mass of the oils after separation from the water, and m_1 is the mass of the oils before mixing. The separation efficiency of modified DAFs was calculated to be greater than 93%, as illustrated in Fig. 8f.

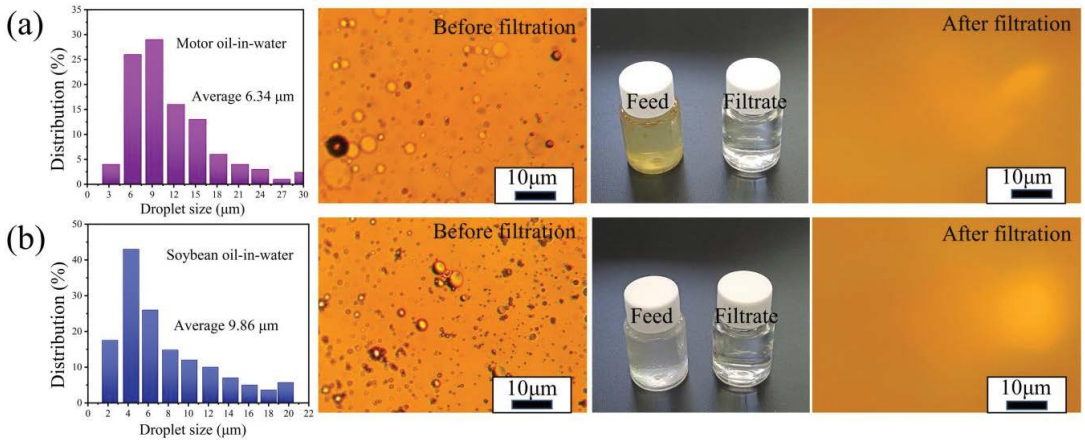

Fig. 7. The size distribution of dispersed droplets, optical micrographs of the feed, and the corresponding filtrate in the separation of (a) the soybean oil/water emulsion and (b) motor oil/water emulsion.

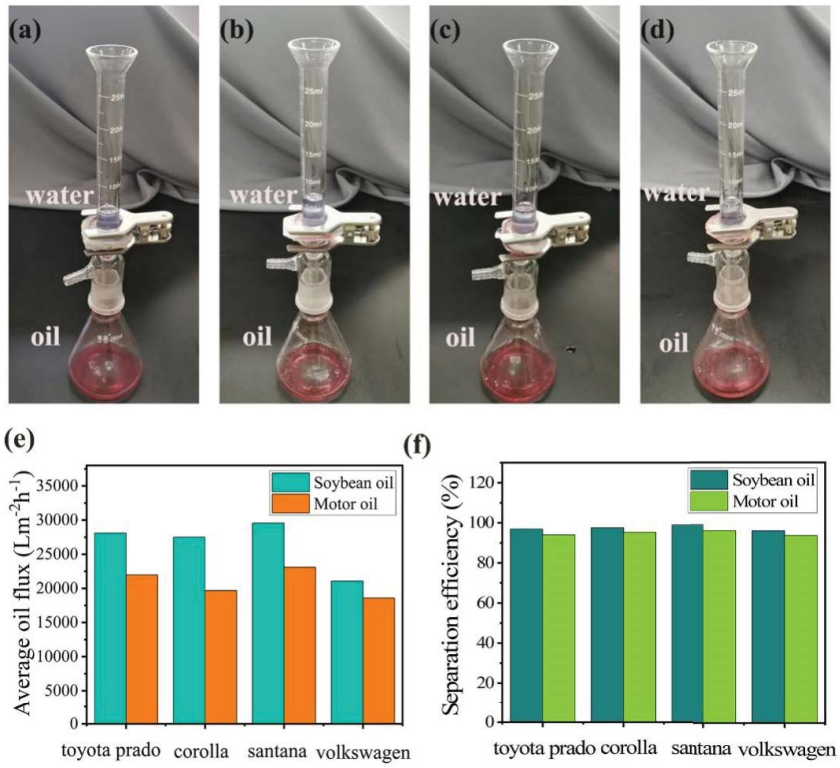

Fig. 8. Digital photographs of separation of oil/water mixtures using various DAFs: (a) Toyota Prado, (b) Corolla, (c) Santana, and (d) Volkswagen, (e) average oil flux of different DAFs and (f) separation efficiencies of various DAFs.

3.4. Mechanism analysis

To understand the mechanism of the superhydrophobicity of the modified DAFs, Fig. 9 depicts a schematic illustration of the water droplet on the coating surface. Cassie and Baxter addressed the phenomenon of solid-liquid contact on a rough solid surface, the equation was proposed to calculate the contact angle of a liquid on a solid surface. In the Cassie–Baxter condition, water droplets remain on the DAF surface [41]. The surface's apparent contact angle on the surface θ_r can be characterized as Eq. (3),

$$\mathrm{Cos}\theta_r = f_1\mathrm{Cos}\theta - f_2 \tag{3}$$

where θ_r and θ are WCAs on rough and flat DAFs modified with the same composition, respectively. f_1 and f_2 are the area proportion of water in contact with solids and air,

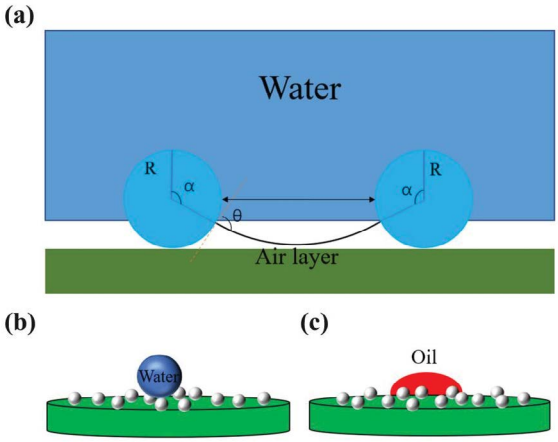

Fig. 9. (a) Schematic diagram of the filtration process of the air filter coated with TiO_2/PDMS at the wetting condition. The mesh shows (b) superhydrophobicity and (c) superoleophilicity states.

respectively ($f_1 + f_2 = 1$). In our line of employment, θ_r and θ is 162° and 94° (Fig. 9), respectively. To better understand the membrane separation property, we examined the creation of the wetting state of the membrane and the influence of the wetting state on separation performance extensively. Based on Eq. (3), it can be calculated that f_2 is 0.946, illustrating that the air fraction trapped between the nanostructures is sufficient to generate superhydrophobicity. Because of PDMS modification, the TiO_2 coated DAFs were covered by a significant number of hydrophobic groups, causing water droplets to linger on the membrane and remain superhydrophobic in Fig. 9a. At the same time, nanostructures can enhance oleophilicity in addition to being oleophilic in nature. As a result, when oil droplets come into contact with the air filter, the capillary action caused by the nanostructures might result in superoleophilicity (Fig. 9c). According to the above, the modified DAFs with superhydrophobic/superoleophilic properties allows oil to flow through the nanosized holes while retaining water droplets.

4. Conclusions

In summary, we have developed a facile and environmentally friendly strategy for producing superhydrophobic DAFs to separate oil-water mixtures under solely gravity driving conditions. The DAFs modified with PDMS and TiO_2 nanoparticles exhibited a high water contact angle of 163° ± 0.3° and good stability in acidic, alkaline, and salt environments. The separation efficiency for heavy oil/water and light oil/water mixes is higher than 96% for ten cycles. This reutilization of DAFs can relieve air filter pollution in environments and turn DAFs into valuable, usable materials. The method provides an effective strategy for effectively treating various oily wastewaters.

Author contributions

Jian-Hua Wei: Conceptualization, Methodology, Xiangchen Li: Visualization, Investigation, Wei-Guo Yan: Review & Editing, Congcong Shen: Formal analysis & Data Curation and Zhifeng Liu: Supervision, Project administration &Funding acquisition.

References

[1] Y. Si, Z. Dong, L. Jiang, Bioinspired designs of superhydrophobic and superhydrophilic materials, ACS Cent. Sci., 4 (2018) 1102–1112.
[2] Q. Ma, H. Cheng, A.G. Fane, R. Wang, H. Zhang, Recent development of advanced materials with special wettability for selective oil/water separation, Small, 12 (2016) 2186–2202.
[3] J. Li, R. Kang, X. Tang, H. She, Y. Yang, F. Zha, Superhydrophobic meshes that can repel hot water and strong corrosive liquids used for efficient gravity-driven oil/water separation, Nanoscale, 8 (2016) 7638–7645.
[4] J.-J. Li, L.-T. Zhu, Z.-H. Luo, Electrospun fibrous membrane with enhanced swithchable oil/water wettability for oily water separation, Chem. Eng. J., 287 (2016) 474–481.
[5] Z. Chu, Y. Feng, S. Seeger, Oil/water separation with selective superantiwetting/superwetting surface materials, Angew. Chem. Int. Ed., 54 (2015) 2328–2338.
[6] Z. Xue, Y. Cao, N. Liu, L. Feng, L. Jiang, Special wettable materials for oil/water separation, J. Mater. Chem. A, 2 (2014) 2445–2460.
[7] N. Marchettini, R. Ridolfi, M. Rustici, An environmental analysis for comparing waste management options and strategies, Waste Manage., 27 (2007) 562–571.
[8] W. Liu, Q. Wang, Q. Peng, Research on Oil Spill Emergency Disposal Technology, Z. Qu, J. Lin, Eds., Proceedings of the International Field Exploration and Development Conference Springer Singapore, Singapore, 2017, pp. 1445–1459.
[9] S.E. Allan, B.W. Smith, K.A. Anderson, Impact of the deepwater horizon oil spill on bioavailable polycyclic aromatic hydrocarbons in Gulf of Mexico coastal waters, Environ. Sci. Technol., 46 (2012) 2033–2039.
[10] C. Chen, W.Z. Xu, P.A. Charpentier, SiO_2 encapsulated TiO_2 nanotubes and nanofibers for self-cleaning polyurethane coatings, J. Photochem. Photobiol., A, 348 (2017) 226–237.
[11] Q.B. Thai, D.K. Le, N.H.N. Do, P.K. Le, P.-T. Nhan, C.Y. Wee, H.M. Duong, Advanced aerogels from waste tire fibers for oil spill-cleaning applications, J. Environ. Chem. Eng., 8 (2020) 104016, doi: 10.1016/j.jece.2020.104016.
[12] X. Li, M. Wang, C. Wang, C. Cheng, X.F. Wang, Facile immobilization of Ag nanocluster on nanofibrous membrane for oil/water separation, ACS Appl. Mater. Interfaces, 6 (2014) 15272–15282.
[13] L.Y. Li, J.F. Zhu, Z.X. Zeng, New approach for recycling office waste paper: an efficient and recyclable material for oily wastewater treatment, ACS Appl. Mater. Interfaces, 12 (2020) 55894–55902.
[14] X.W. Ruan, T.C. Xu, D.J. Chen, Z.W. Ruan, H.T. Hu, Superhydrophobic paper with mussel-inspired polydimethylsiloxane-silica nanoparticle coatings for effective oil/water separation, RSC Adv., 10 (2020) 8008–8015.
[15] S.T. Nguyen, J.D. Feng, N.T. Le, A.T.T. Le, N. Hoang, V.B.C. Tan, H.M. Duong, Cellulose aerogel from paper waste for crude oil spill cleaning, Ind. Eng. Chem. Res., 52 (2013) 18386–18391.
[16] G. Demirel Bayık, A. Altın, Production of sorbent from paper industry solid waste for oil spill cleanup, Mar. Pollut. Bull., 125 (2017) 341–349.
[17] M. Likon, F. Černec, F. Švegl, J. Saarela, T.F. Zimmie, Papermill industrial waste as a sustainable source for high efficiency absorbent production, Waste Manage., 31 (2011) 1350–1356.
[18] J.X. Ai, Z.G. Guo, Facile preparation of a superamphiphobic fabric coating with hierarchical TiO_2 particles, New J. Chem., 44 (2020) 19192–19200.
[19] L.F. Yu, S.M. Zhang, M. Zhang, J.D. Chen, Superhydrophobicity construction with dye-sensitised TiO_2 on fabric surface for both oil/water separation and water bulk contaminants purification, Appl. Surf. Sci., 425 (2017) 46–55.
[20] R.J. Li, L.H. Rao, J.Z. Zhang, L.G. Shen, Y.C. Xu, X.J. You, B.-Q. Liao, H.J. Lin, Novel *in-situ* electroflotation driven

by hydrogen evolution reaction (HER) with polypyrrole (PPy)-Ni-modified fabric membrane for efficient oil/water separation, J. Membr. Sci., 635 (2021) 119502, doi: 10.1016/j.memsci.2021.119502.
[21] W.X. Chao, S.B. Wang, Y.D. Li, G.L. Cao, Y.S. Zhao, X.H. Sun, C.Y. Wang, S.-H. Ho, Natural sponge-like wood-derived aerogel for solar-assisted adsorption and recovery of high-viscous crude oil, Chem. Eng. J., 400 (2020) 125865, doi: 10.1016/j.cej.2020.125865.
[22] R. Yang, Q.H. Cao, Y.Y. Liang, S. Hong, C.L. Xia, Y.J. Wu, J.Z. Li, L.P. Cai, C. Sonne, Q.V. Le, S.S. Lam, High capacity oil absorbent wood prepared through eco-friendly deep eutectic solvent delignification, Chem. Eng. J., 401 (2020) 126150, doi: 10.1016/j.cej.2020.126150.
[23] Y.J. Cai, Y. Wu, F. Yang, J. Gan, Y.J. Wang, J.L. Zhang, Wood sponge reinforced with polyvinyl alcohol for sustainable oil-water separation, ACS Omega, 6 (2021) 12866–12876.
[24] K.L. Wang, X.R. Liu, Y. Tan, W. Zhang, S.F. Zhang, J.Z. Li, Two-dimensional membrane and three-dimensional bulk aerogel materials via top-down wood nanotechnology for multibehavioral and reusable oil/water separation, Chem. Eng. J., 371 (2019) 769–780.
[25] W.M. Liu, M.K. Cui, Y.Q. Shen, G.R. Zhu, L. Luo, M.J. Li, J. Li, Waste cigarette filter as nanofibrous membranes for on-demand immiscible oil/water mixtures and emulsions separation, J. Colloid Interface Sci., 549 (2019) 114–122.
[26] C. Liu, B.B. Chen, J. Yang, C.S. Li, One-step fabrication of superhydrophobic and superoleophilic cigarette filters for oil-water separation, J. Adhes. Sci. Technol., 29 (2015) 2399–2407.
[27] A. Doyan, C.L. Leong, M.R. Bilad, K.A. Kurnia, S. Susilawati, S. Prayogi, T. Narkkun, K. Faungnawakij, Cigarette butt waste as material for phase inverted membrane fabrication used for oil/water emulsion separation, Polymers, 13 (2021) 1907, doi: 10.3390/polym13121907.
[28] J.L. Zhang, H. Xu, J. Guo, T.C. Chen, H.T. Liu, Superhydrophobic polypyrrole-coated cigarette filters for effective oil/water separation, Appl. Sci., 10 (2020) 1985, doi: 10.3390/app10061985.
[29] M. Bartmański, Ł. Pawłowski, A. Zieliński, A. Mielewczyk-Gryń, G. Strugała, B. Cieślik, Electrophoretic deposition and characteristics of chitosan–nanosilver composite coatings on a nanotubular TiO_2 layer, Coatings, 10 (2020) 245, doi: 10.3390/coatings10030245.
[30] B.Y.L. Tan, J. Juay, Z.Y. Liu, D. Sun, Flexible hierarchical TiO_2/Fe_2O_3 composite membrane with high separation efficiency for surfactant-stabilized oil-water emulsions, Chem. An Asian J., 11 (2016) 561–567.
[31] L. Zhang, X. Yang, B. Jiang, Y. Sun, Z. Gong, N. Zhang, S. Hou, J. Li, N. Yang, Superhydrophilic and underwater superoleophobic Ti foam with robust nanoarray structures of TiO_2 for effective oil-in-water emulsion separation, Sep. Purif. Technol., 252 (2020) 117437, doi: 10.1016/j.seppur.2020.117437.
[32] Z.-h. Zhang, H.-j. Wang, Y.-h. Liang, X.-j. Li, L.-q. Ren, Z.-q. Cui, C. Luo, One-step fabrication of robust superhydrophobic and superoleophilic surfaces with self-cleaning and oil/water separation function, Sci. Rep., 8 (2018) 3869, doi: 10.1038/s41598-018-22241-9.
[33] H. Bellanger, T. Darmanin, E.T. de Givenchy, F. Guittard, Chemical and physical pathways for the preparation of superoleophobic surfaces and related wetting theories, Chem. Rev., 114 (2014) 2694–2716.
[34] B. Wang, Y. Zhang, L. Shi, J. Li, Z. Guo, Advances in the theory of superhydrophobic surfaces, J. Mater. Chem., 22 (2012) 20112–20127.
[35] D. Sriramulu, E.L. Reed, M. Annamalai, T.V. Venkatesan, S. Valiyaveettil, Synthesis and characterization of superhydrophobic, self-cleaning NIR-reflective silica nanoparticles, Sci. Rep., 6 (2016) 35993, doi: 10.1038/srep35993.
[36] P. Khanjani, A.W.T. King, G.J. Partl, L.-S. Johansson, M.A. Kostiainen, R.H.A. Ras, Superhydrophobic paper from nanostructured fluorinated cellulose esters, ACS Appl. Mater. Interfaces, 10 (2018) 11280–11288.
[37] L. Qiu, J.X. Zhang, Z.G. Guo, W.M. Liu, Asymmetric superwetting stainless steel meshes for on-demand and highly effective oil-water emulsion separation, Sep. Purif. Technol., 273 (2021) 118994, doi: 10.1016/j.seppur.2021.118994.
[38] S.N. Li, L. Zhong, S. Huang, D.F. Wang, F.X. Zhang, G.X. Zhang, A reactive fluorine-free, efficient superhydrophobic and flame-retardant finishing agent for cotton fabrics, Cellulose, 26 (2019) 6333–6347.
[39] B. Bolvardi, J. Seyfi, I. Hejazi, M. Otadi, H.A. Khonakdar, S.M. Davachi, Towards an efficient and durable superhydrophobic mesh coated by PDMS/TiO_2 nanocomposites for oil/water separation, Appl. Surf. Sci., 492 (2019) 862–870.
[40] M.P. Yang, C. Jiang, W.Q. Liu, L.Y. Liang, K. Pi, A less harmful system of preparing robust fabrics for integrated self-cleaning, oil-water separation and water purification, Environ. Pollut., 255 (2019) 113277, doi: 10.1016/j.envpol.2019.113277.
[41] A.B.D. Cassie, S. Baxter, Wettability of porous surfaces, Trans. Faraday Soc., 40 (1944) 546–551.